THERMAL ANALYSIS OF TRAPEZOIDAL GROOVED HEAT-PIPE EVAPORATOR WALLS

G. E. Schneider* and M. M. Yovanovich+

University of Waterloo, Waterloo, Ontario

and

V. A. Wehrle±

Communications Research Centre, Ottawa, Ontario

Abstract

A model is proposed for heat-pipe analysis which accounts for the influence of the liquid/metal matrix in a trapezoidal grooved evaporator wall through the use of an equivalent heat-transfer coefficient. A conduction model is used with the free surface specified to be at the saturation temperature. The problem is solved using the finite-element method, and a parametric study was conducted for a wide range of the geometric and thermal parameters. A correlation of the results is presented, and a comparison is made with existing theoretical and experimental results.

Nomenclature

A, A_1, A_2	= correlation parameters
B, B_1, B_2, B_3	= correlation parameters
d	= groove depth
h_{eq}	= equivalent heat-transfer coefficient
H	= typical cell height
k_f, k_m	= fluid and metal thermal conductivities
n	= normal to solid/liquid interface

Presented as Paper 76-481 at the AIAA 11th Thermophysics Conference, San Diego, Calif., July 14-16, 1976.

*Project Engineer.

+Professor, Thermal Engineering Group, Department of Mechanical Engineering.

±Staff Engineer.

N	= groove pitch, number per lineal distance
NE1,NE2, ND,NW,NF	= finite-element mesh parameters
Nu_f	= equivalent Nusselt number, Equation (5)
q	= surface heat flux
T	= temperature
T^*	= temperature excess, $T^* = T - T_v$
T_f, T_m	= fluid and metal temperature distributions
T_s	= groove root temperature
T_v	= vapor temperature
w	= width of typical analysis cell
x	= Cartesian coordinate
x_α	= normalized contact angle, $x_\alpha = \alpha/(\pi/2 - \theta_o)$
y	= Cartesian coordinate
α	= apparent contact angle
ε_1	= groove land width
ε_2	= groove root width
θ_o	= groove half-angle

Superscript

*	= nondimensionalization with respect to w except as noted previously for T^*

Introduction

In the analysis and design of heat pipes in their role as a thermal energy transport device, it is imperative, for successful incorporation of the heat pipe into an overall thermal system, that its operating characteristics be known. Not only must performance limits be established to enable accurate analysis, but also the heat-transfer performance of the device during operation must be determined. Of importance in determining heat-pipe performance characteristics are the temperature drops experienced at the pipe inner surface as a result of heat transfer to and from the pipe interi in the evaporator and condenser regions, respectively.

The work being reported in this paper is directed at the prediction of the evaporator inner surface heat-transfer characteristics. Analysis of the condenser heat-transfer characteristics requires a treatment different from that for the evaporator and has been investigated previously by Kamotani.[1] This work considers evaporator grooves having a general trapezoidal cross section, whose limiting geometries are the sharp V-groove and the rectangular groove, and which will be applicable to the design and analysis of many moderate and high-capacity heat-pipe configurations.

As noted by Edwards et al.,[2] the benefits to be gained through the use of grooved surfaces are substantial. Carnavos,[3] for example, reported evaporation side heat-transfer coefficients ranging from 3000 to 7000 Btu/hr-ft^2°F. Although much experimental work has been done on this subject, only several theoretical analyses have been reported.[2,4,5]

A model is proposed in this paper for determination of the heat-transfer characteristics for evaporator surfaces which include the influence of heat conduction within the wall material of the groove "fin" region. The heat-transfer characteristics are examined for a range of materials combinations and groove cross sections of practical utility to the heat-pipe community.

Analysis

Equivalent Heat-Transfer Coefficient

The cross section of a grooved-heat-pipe wall is illustrated schematically in Fig. 1a for the case of a sharp V-groove. In examining the thermal problem associated with heat transfer across this wall, the conservation equations must be solved for the entire region, including the detailed region where the liquid/wall matrix exists. Experience in conduction heat-transfer analysis indicates, however, that substantial addition of pipe wall material, for wall thicknesses of the same order as the groove spacing, will be reflected as an addition of a pure conductive resistance in

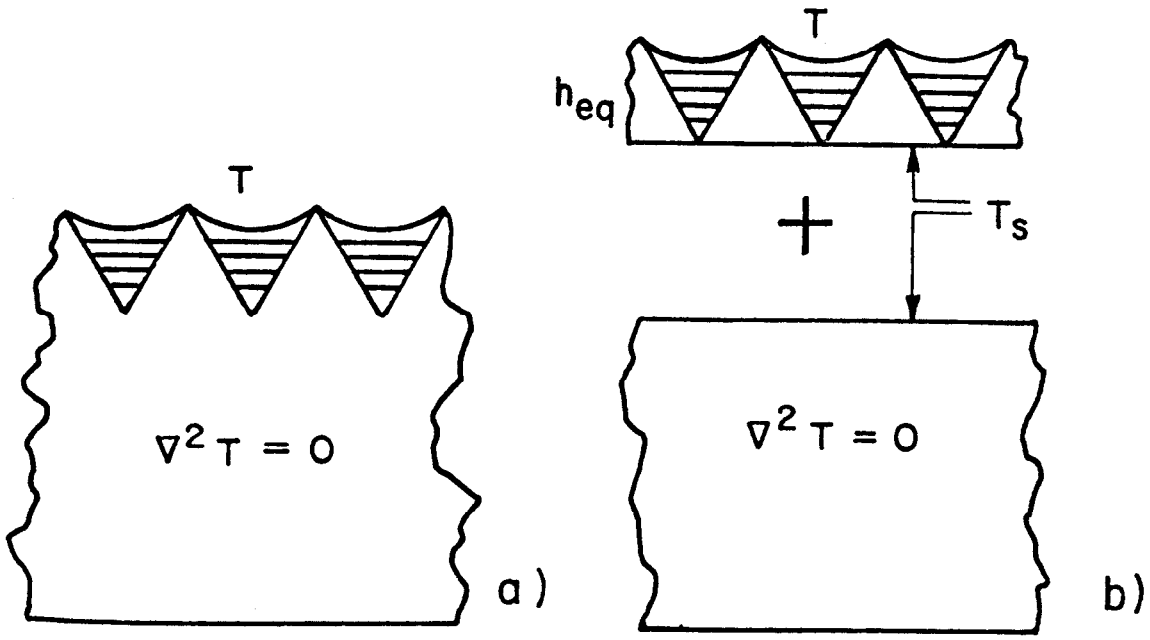

Fig. 1 Problem geometry illustrating the equivalent heat-transfer coefficient.

series with the system to which it is added. It is in recognition of this behavior that the equivalent heat-transfer coefficient is introduced.[6,7] This enables the heat-transfer characteristics of a given grooved-heat-pipe wall to be extended to other heat-pipe walls having similar groove geometries but different wall thicknesses.

The use of the equivalent heat-transfer coefficient is illustrated in Fig. 1b. A hypothetical surface is constructed at the groove root surface, and the equivalent heat-transfer coefficient is applied over this surface. Its determination is effected by solving the complete composite problem, including the pipe wall, and subtracting from the total resistance the one-dimensional resistance of the pipe wall. In this way, the equivalent heat-transfer coefficient is used to account for the influence of the groove liquid/fin matrix and can be applied to walls having different pipe wall thicknesses.

Mathematical Formulation of the Problem

The liquid cross section at any station in the pipe groove is determined by consideration of the liquid flow hydrodynamics. In many situations, quasiestablished heat-transfer and fluid-flow conditions can be assumed, and several analyses are available which make use of these assumptions to establish the liquid cross-section variation within the grooves.[2,3,6-10] This analysis assumes that the liquid cross section has been determined appropriately and examines the remaining heat-transfer problem. The heat-transfer problem is examined under the following assumptions:

1) The radius of curvature of the free surface meniscus is constant.

2) The heat-transfer conditions are quasiestablished at each groove cross section.

3) Liquid convection does not contribute significantly to the heat transfer.

4) Nonequilibrium effects at the free surface can be neglected.

5) The temperature of the free surface is uniform at the saturation temperature corresponding to the vapor pressure.

6) Steady-state conditions prevail.

Under the preceding assumptions, the problem becomes one of pure heat conduction from the pipe outer wall, through the wall, and through the liquid/solid matrix to the vapor

core. This is consistent with previous investigations.[2,5-7,11] In addition, it is assumed that the liquid cross section variation between adjacent grooves is sufficiently small that the midplane between grooves can be considered to be adiabatic. This assumption, also consistent with previous analyses,[2,5-7,11] permits examination of a "typical cell" as illustrated in Fig. 2.

A Cartesian coordinate system is established as illustrated in the figure with liquid and metal thermal conductivities of k_f and k_m in their respective regions of the cross section. The groove land width is denoted by ϵ_1 and the groove root width by ϵ_2. The geometry of Fig. 2 readily degenerates to the two limiting cases commonly employed in heat-pipe designs: $\epsilon_1 = \epsilon_2 = 0$ for the sharp V-groove and $\epsilon_1 = \epsilon_2 = 0.5$ for the rectangular groove. Grooves of symmetric cross section are considered in this work.

The liquid/vapor interface is assumed uniform at the saturation value, whereas, because of the low relative thermal conductivity of the vapor space, the exposed groove land area is assumed to be adiabatic. The lateral boundaries of the cell also are given an insulative specification. Over the pipe wall exterior surface, a uniform heat flux is applied.

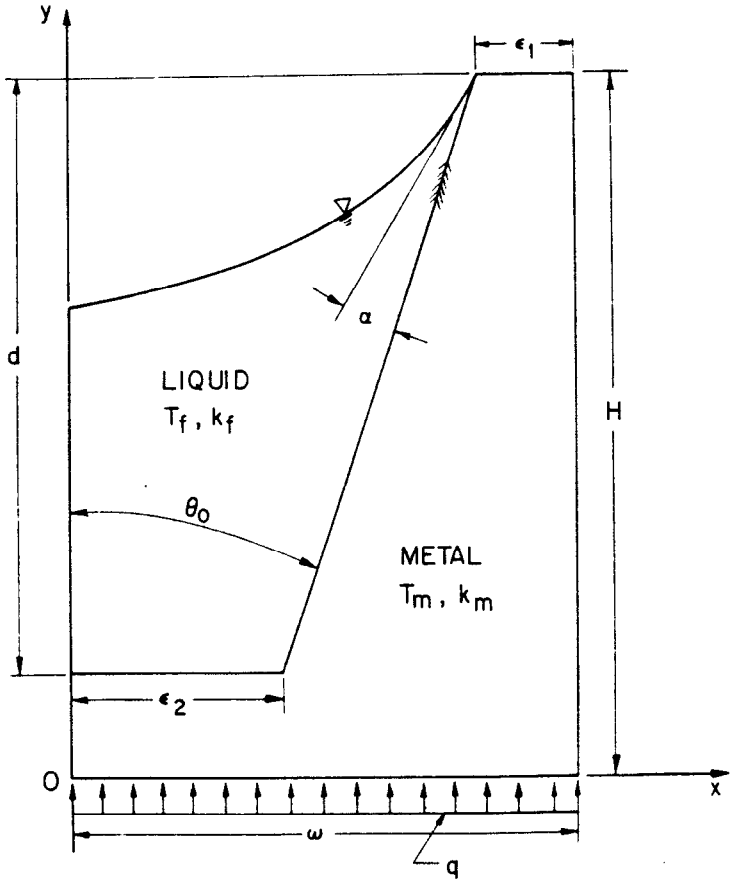

Fig. 2 Typical cell for analysis.

Defining a temperature excess by

$$T^* \equiv T - T_v \tag{1}$$

and normalizing the length scales with respect to the cell width w, the governing differential equation can be written as

$$\frac{\partial^2 T_f^*}{\partial x^{*2}} + \frac{\partial^2 T_f^*}{\partial y^{*2}} = 0 \tag{2}$$

for the metal region. The solution to Eqs. (2) and (3) must satisfy the following boundary conditions:

for the liquid region, and

$$\frac{\partial^2 T_m^*}{\partial x^{*2}} + \frac{\partial^2 T_m^*}{\partial y^{*2}} = 0 \tag{3}$$

$$y^* = 0,\ 0 \le x^* \le 1;\ \frac{\partial T^*}{\partial y^*} = \frac{-qw}{k_m} \tag{4a}$$

$$y^* = H^* - d^*,\ 0 \le x^* \le \varepsilon_2;\ k_m \frac{\partial T_m^*}{\partial y^*} = k_f \frac{\partial T_f^*}{\partial y^*} \tag{4b}$$

$$y^* = (H^* - d^*) + \frac{d^*(x^* - \varepsilon_2^*)}{1 - \varepsilon_1^* - \varepsilon_2^*},\ \varepsilon_2^* \le x^* \le 1 - \varepsilon_1^*;\ k_m \frac{\partial T_m^*}{\partial n^*} = k_f \frac{\partial T_f^*}{\partial n^*} \tag{4c}$$

$$y^* = H^*,\ 1 - \varepsilon_1^* \le x^* \le 1;\ \frac{\partial T_m^*}{\partial y^*} = 0 \tag{4d}$$

$$x^* = 0,\ 0 \le y^* \le H^* - d^*;\ \frac{\partial T_m^*}{\partial x^*} = 0 \tag{4e}$$

$$x^* = 0,\ H^* - d^* \le y^* \le y_i^*(0);\ \frac{\partial T_f^*}{\partial x^*} = 0 \tag{4f}$$

$$y^* = y_i^*(x),\ 0 \le x^* \le 1 - \varepsilon_1^*:\ T_f^*[x^*, y_i^*(x^*)] = 0 \tag{4g}$$

$$x^* = 1,\ 0 \le y^* \le H^*;\ \frac{\partial T_m^*}{\partial x^*} = 0 \tag{4h}$$

In the foregoing, n^* is the outward normal to the metal region at the metal/liquid interface, and $y_i^*(x^*)$ represents the geometric description of the free surface. Clearly, an

analytical solution to Eqs. (2) and (3) which satisfies the boundary conditions (4a-4h) is not feasible using currently available analytical methods. In view of this, it was decided to use a numerical solution method to solve the problem.

Numerical Solution

Because of the irregular shape of the solution domain, the method best suited for solution is the finite-element method. This is a result of the geometric flexibility that is available through the use of this method. Although the details of the numerical formulation of this problem using the finite-element method will not be presented in this paper, they can be found in Ref. 7. Linear quadrilateral finite elements were used in the investigation.

Considerable difficulty was experienced during the initial phases of the investigation and is related to the element shapes and their distribution within the solution domain. These types of difficulty are extremely problem-dependent, are difficult to anticipate, and usually are

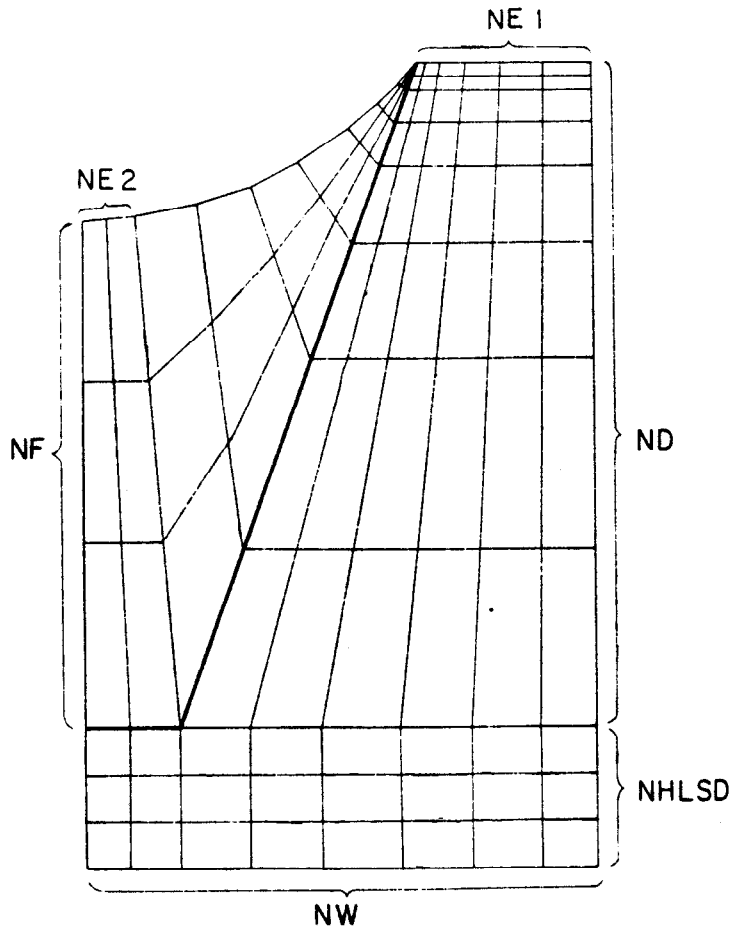

Fig. 3 Finite-element mesh generation scheme, illustrative only.

detected only when examining the solution convergence characteristics. In this regard, the experience gained by the authors indicates that the heat-transfer problem, as modeled in this investigation, is an extremely difficult one.

In the case of moderate-temperature heat pipes, the working fluid is typically of low thermal conductivity, e.g., water, methanol, ammonia, etc., whereas the pipe structure, typically metallic, has a high thermal conductivity, e.g., stainless steel, carbon steel, aluminum, copper etc. The conductivity ratio k_f/k_m for these combinations therefore can range from 0.03 for water/stainless steel pipes to 0.0014 for methanol/copper pipes, and enforcing the interface compatibility requirements is difficult except for problems of simple geometry.

Furthermore, the preceding problem is compounded by the geometric characteristics of the trapezoidal groove problem for two reasons. First, the liquid-free surface is such that, at the meniscus attachment point, the liquid thickness vanishes. This results in an extremely local region over which the bulk of the heat transfer is concentrated. Typically, in excess of 90% of the heat transfer occurs near the meniscus contact, over an area measuring only several percent of the total. The second reason, compounding the first, is that the metal section extends fully to the vapor core. This affords the heat flow a low resistance path to the meniscus contact region and further concentrates the heat flow in this region. A viable solution program therefore must be sufficiently flexible to "pick up" the large gradients existing near the meniscus contact and to blend this region into the remaining portion of the solution domain, where the heat flow is less concentrated and gradients are smaller. After two mesh-generation schemes were applied and proved unsatisfactory, a third was devised which provides monotone, asymptotic convergence as the number of nodal points used in the discretized solution domain is increased.

The discretized solution domain is illustrated schematically in Fig. 3. The element distribution is arranged such that the predominant heat-flow direction is normal to the element long side, thereby enabling the solution to detect rapid changes in the local gradient. This is particularly important in the fluid region near the meniscus contact. In addition, a nonlinear gradation of element size was employed to provide a high degree of mesh refinement in the vicinity of the meniscus attachment at the wall in both the liquid and metal regions. Typical values of the

parameters appearing in Fig. 3 used for a "converged" solution are NE1 = 19, NE2 = 6, ND = 52, NW = 25, and NF = 10, providing 1743 elements with 1828 degrees of freedom.

Solution Accuracy

The convergence characteristics of the numerical solution procedure adopted in this work are presented in Fig. 4 for the case where $k_f/k_m = 0.001$, $\theta_o = 20°$, $x_\alpha \equiv \alpha/(\pi/2 - \theta_o)] = 0.05$, and $\varepsilon_1 = \varepsilon_2 \equiv 0.25$. The ordinate of the curve is $Nu_f \cdot k_f/k_m$, where the equivalent Nusselt number Nu_f is defined as

$$Nu_f \equiv h_{eq}/Nk_f \tag{5}$$

where N is the number of grooves per unit length of wall cross section. This combination of parameters represents a severe test for the solution algorithm, since the apparent contact angle is small and the conductivity ratio is extreme. Convergence was achieved more rapidly for less severe parameter combinations. The convergence is seen to be both monotone and asymptotic to a limiting value.

Anticipating that the convergence curve follows an inverse dependence on the number of nodal degrees of freedom, the hyperbolic conic section was used to examine the convergence behavior. Correlation of the numerical data with a hyperbolic curve using a least-squares minimization procedure yielded an extrapolated asymptote that is only 1.96% removed from the final numerical data point. The maximum error of this correlation over the entire range was 1.4%. Adding these two influences indicates that a solution error in the final data point of approximately 3.36% can be expected. The solution therefore is expected to be within 5% of the

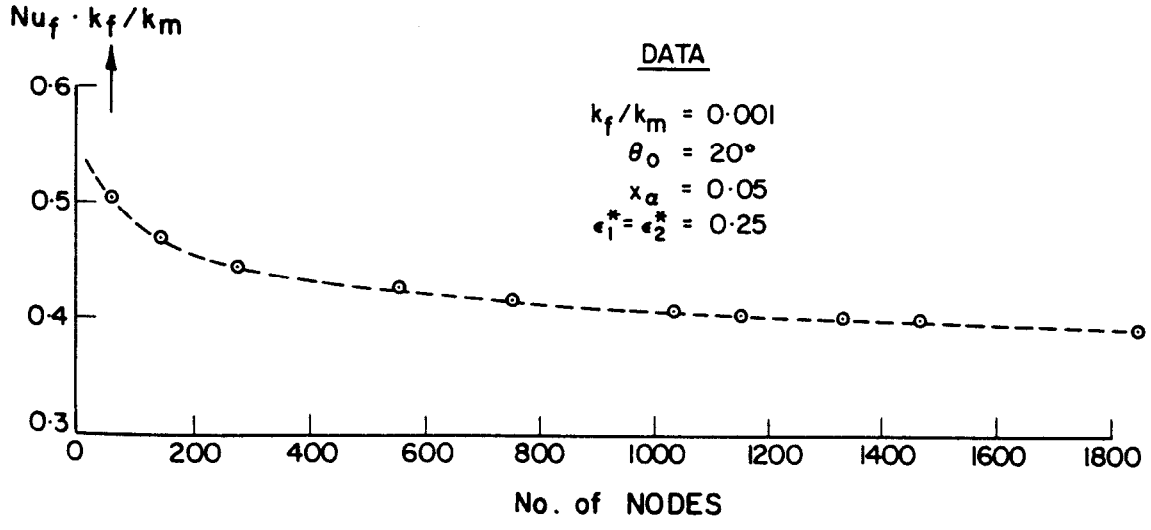

Fig. 4 Convergence characteristics of finite-element solution.

Table 1 Parameter values used in parametric study

k_f/k_m	$d^*=d/w$	$\varepsilon_1^*=\varepsilon_2^*$	x_α
0.1	1.0	0.01	0.05
0.01156	1.5	0.25	0.25
0.001	2.0	0.49	0.50
			1.00

true value, with higher accuracy anticipated for the less severe parameter combinations.

In further support of the numerical solution procedure, a situation was examined for which an analytic solution is available. This limiting case is that for which the groove is in a full condition, $\alpha + \theta_o = \pi/2$, and for which the conductivity ratio k_f/k_m is unity. The case for which $\varepsilon_1 = \varepsilon_2 = 0.25$ was examined numerically for a dimensionless thickness H^* of 1.4737, the analytic solution of which can be determined using the elliptic integrals of the first kind following the procedure outlined in Refs. 7 and 12. The numerical solution obtained for this limiting case agrees to within 0.15% of the analytic solution and supports the correct operation of the finite-element prediction program.

Results

Restricting the analysis to grooves of symmetric cross section, $\varepsilon_1^* = \varepsilon_2^*$, the thermal problem is characterized by four parameters: the conductivity ratio k_f/k_m, the normalized apparent contact angle $x_\alpha = \alpha/(\pi/2 - \theta_o)$, the groove depth in relation to the cell width $d^* = d/w$, and the land area ratio $\varepsilon_1^* = \varepsilon_2^*$. Numerical solutions were obtained for the combinations of parameters presented in Table 1.

A typical set of results is presented in Fig. 5 for the case where $\varepsilon_1^* = \varepsilon_2^* = 0.01$, corresponding to the V-groove configuration, and for a conductivity ratio, $k_f/k_m = 0.01156$, corresponding to a stainless-steel/methanol heat pipe. As anticipated, all of the numerical results exhibit a monotone, decreasing dependence of the quantity $Nu_f \cdot k_f/k_m$ on the normalized apparent contact angle x_α. This character is due to the low thermal conductivity of the liquid working fluid and results in a preferential migration of the heat flow

through the metal toward the meniscus contact region, where the liquid thickness is the smallest. Since the local liquid thickness decreases with decreasing contact angle, the conductance is higher for the low contact angle situations. This trend is not as pronounced, however, as that noted in previous investigations.[2,6] Indeed, the dependence on apparent contact angle was noted to be more pronounced for the more closely matched thermal conductivity situation, since here the bulk liquid section plays a more active role in the thermal exchange.

For consideration of parameter combinations different from those presented in Fig. 5, the correlation equation is provided:

$$Nu_f.k_f/k_m = A\ \ell n(x_\alpha) + B \tag{6}$$

where

$$A = A_1[-0.389\ d^* + 1]\varepsilon^* + A_2[-0.376\ d^* + 1] \tag{7a}$$

$$B = B_1[-0.29\ d^* + 1]\varepsilon^{*2} + B_2[-0.228\ d^* + 1]\varepsilon^* + B_3[5.368\ \exp(-1.295\ d^*) + 1] \tag{7b}$$

and

$$A_1 = 0.0056\ \ell n^2(k_f/k_m) + 0.1025\ \ell n(k_f/k_m) + 0.4511 \tag{8a}$$

$$A_2 = -0.0098\ \ell n^2(k_f/k_m) - 0.1413\ \ell n(k_f/k_m) - 0.5251 \tag{8b}$$

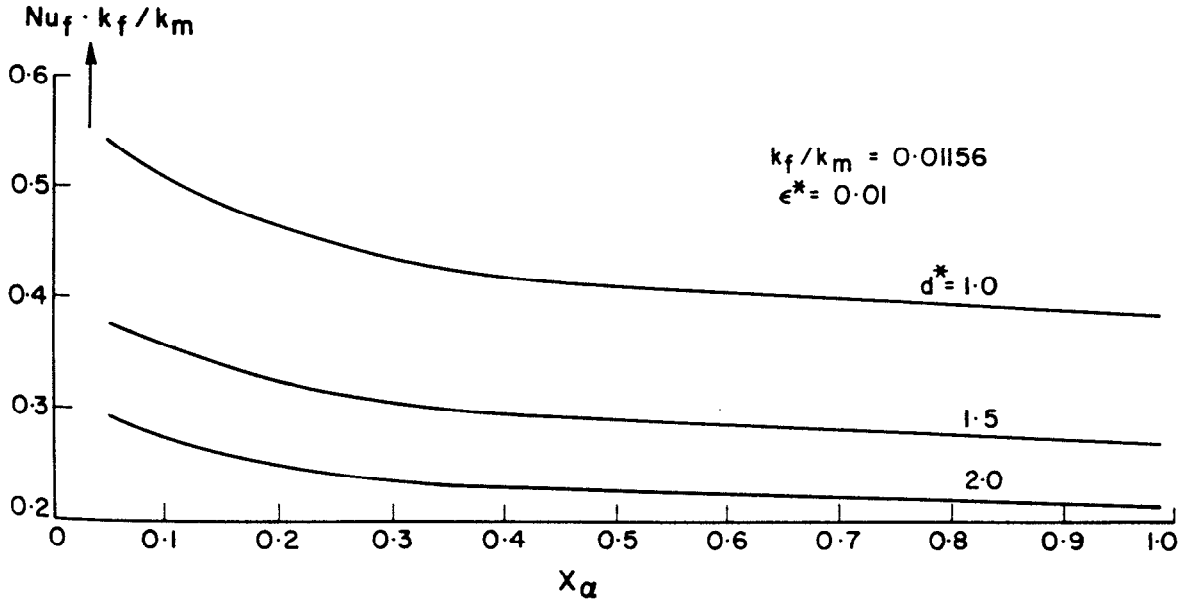

Fig. 5 Numerical results for $\varepsilon_1^* = \varepsilon_2^* = 0.01$, $k_f/k_m = 0.0116$.

$$B_1 = 0.0336\ \ell n^2(k_f/k_m)+0.4557\ \ell n(k_f/k_m)-1.0821 \quad (8c)$$

$$B_2 = -0.0407\ \ell n^2(k_f/k_m)-0.5090\ \ell n(k_f/k_m)-0.2668 \quad (8d)$$

$$B_3 = 0.0105\ \ell n^2(k_f/k_m)+0.1254\ \ell n(k_f/k_m)+0.4986 \quad (8e)$$

The preceding correlation equation correlates all of the numerical data for the parameter combinations indicated in Table 1. The largest errors of correlation, up to 7%, occur for the conductivity ratio of 0.1. Otherwise, correlation is everywhere within 5%.

A second trend, consistent with the problem physics, is that the heat transfer decreases with increasing groove depth. The major adjustment of the thermal flowfield occurs in the region near the meniscus contact, and consequently, in the remainder of the metal fin portion, the flowfield is quasiuniform. As a result, the influence of increasing d^* is to add a section of pure conductive, variable-area metal to that for the case of smaller groove depth. A secondary influence of increasing the groove depth for a fixed land area ratio is that the problem geometry necessarily is altered. The associated change in θ_o affects the actual apparent contact angle through the definition of the normalized apparent contact angle, $x_\alpha = \alpha/(\pi/2-\theta_o)$.

The influence of the conductivity ratio is to decrease the product $Nu_f.k_f/k_m$ as the conductivity ratio is decreased. This is a result of the higher heat-flow concentration experienced at the groove tip due to the decreased liquid thermal conductivity.

The influence of changing land area ratio, however, is not monotonic as in the previous cases, but rather produces a maximum value near a land area ratio of $\varepsilon_1^* = \varepsilon_2^* = 0.25$. Exception to this occurs at small apparent contact angles for a conductivity ratio of $k_f/k_m \doteq 0.1$. The geometric changes incurred by the variation of ε^* are severe, and it is difficult to anticipate precisely the influence of this parameter on the overall heat transfer, since these geometric changes influence both the liquid and metal region geometries. It is felt that the observed maximum is the result of a favorable balance between the changing pure conductive resistance and the changing liquid/metal interaction, each of which is changing at a different rate.

Discussion and Conclusions

An equivalent heat-transfer coefficient has been introduced in this investigation in a manner that allows utilization of the results of groove heat-transfer analyses to heat-pipe designs having differing wall thicknesses. The equivalent heat-transfer coefficient, accounting for the influence of the groove/liquid matrix, will enable flexible procedures to be employed in the thermal analysis and design of heat-pipe structures.

A numerical analysis, using the finite-element method, has been performed to determine the equivalent heat-transfer coefficient for grooves of a general trapezoidal cross section. The heat-transfer analysis is based on the conduction model used by previous investigators.[2,5] The results of a numerical study examining the parameter combinations appearing in Table 1 have been presented in the form of a correlation equation. The numerical data points are deemed to be accurate, for the model used, to within +5% (convergence from above), and the correlation equation for the data provides similar accuracy.

A comparison of the present results with the approximate analysis of Edwards et al., not reported in detail here, supports the validity of the numerical results. For a conductivity ratio of 0.1, the maximum departure of the Edwards approximate solution from the present numerical results is 16%. For a conductivity ratio of 0.0116, their approximate solution falls between 3 and 47% below the current work. In their paper,[2] they conducted a comparison with the experimental work of Prince,[13] in which their approximate solution predicted values for the average external groove-side coefficient which fell 18% below the measured value. This is consistent with their solution's departure by a comparable amount from the present results. As the conductivity ratio is decreased, further however, the agreement of the approximate solution with the present results becomes poorer. It is worth noting here that the Edwards[2] analysis, in agreement with the present work, predicts very large heat-transfer coefficients for grooved surfaces which are compatible with the observed coefficients for evaporation from externally grooved surfaces.

Turning our attention to the heat-pipe literature, however, certain discrepancies arise. Berger and Feldman[5] performed a finite-difference solution to determine the heat-transfer characteristics of V-groove and rectangular-groove heat-pipe walls. The model they used is consistent with that used in this investigation. Their results, predicting low heat-transfer coefficients, were in good agreement with the

measured values obtained from heat-pipe experiments available in the literature and reported in their paper.[5] Because of the nature of the difficulties experienced in the present work, resulting from the extremely local flux concentrations near the meniscus contact, and in consideration of the relatively coarse grid employed in their work, the accuracy of their results is held suspect by the present authors. However, the discrepancy still remains that the model and solution, capable of predicting the heat-transfer coefficients for evaporation from externally grooved tubes, appear to be inadequate for the prediction of internal heat-pipe coefficients. Disagreement is observed to approach an order of magnitude under certain circumstances.

Experimentation with the present finite-element code indicates that changing the free surface boundary condition, by forcing a uniform evaporative flux over this surface, can alter the numerical results substantially in excess of an order of magnitude, but, of course, there is no apparent motivation at present for the use of this boundary condition. Resolution of the apparent paradox just indicated is one of extreme importance to the heat-pipe community, and research efforts certainly should be directed at its resolution.

Acknowledgments

The authors gratefully acknowledge the contract support of G.E. Schneider by the Communications Research Centre, Department of Communications, Ottawa, Ontario, Canada. One of the authors (GES) acknowledges many fruitful discussions with G.M. McNeice of the Department of Civil Engineering, University of Waterloo, on matters pertaining to the finite-element code.

References

[1]Kamotani, Y., "Analysis of Axially Grooved Heat Pipe Condensers," AIAA Paper 76-147, Washington, D.C., Jan. 1976; also, elsewhere in this volume.

[2]Edwards, D.K., Gier, K.D., Ayyaswamy, P.S., and Catton, I., "Evaporation and Condensation in Circumferential Grooves on Horizontal Tubes," ASME-AIChE Heat Transfer Conference, ASME Paper 73-HT-25, Atlanta, Ga., Aug. 1973.

[3]Carnavos, T.C., "Thin film Distallation," Proceedings of the First International Symposium on Water Desalination, U.S. Dept. of the Interior, 1965, pp. 205-213.

[4]Edwards, D.K., Balakrishnan, A., and Catton, I., "Power-Law Solutions for Evaporation from a Finned Surface," ASME Journal of Heat Transfer, Vol. 96, 1974, pp. 423-425.

[5]Berger, M.E. and Feldman, K.T., Jr., "Analysis of Circumferentially Grooved Heat Pipe Evaporators," ASME Winter Annual Meeting, ASME Paper 73-WA/HT-13, Detroit, Mich., Nov. 1973.

[6]Schneider, G.E. and Yovanovich, M.M., "Three-Dimensional Thermal Analysis of High Capacity Heat Pipe with Circumferential V-Grooves," Final Rept. to the Communications Research Centre, Dept. of Communications, Ottawa, Ontario, Aug. 1974.

[7]Schneider, G.E. and Yovanovich, M.M., "Thermal Analysis of Trapezoidal Grooved Heat Pipe Walls," Final Rept. to the Communications Research Centre, Dept. of Communications, Ottawa, Ontario, Aug. 1975.

[8]Hsu, W.J., "A Numerical Analysis of Capillary Flow in Trapezoidal Grooves During Evaporation or Condensation," M.S. Thesis, Univ. of California at Los Angeles, 1976.

[10]Gier, K.D. and Edwards, D.K., "Flooding and Dryup Limits of Circumferential Heat Pipe Grooves," Journal of Spacecraft and Rockets, Vol. 12, Sept. 1975, pp. 517-518.

[11]Feldman, K.T., Jr. and Berger, M.E., "Analysis of a High-Heat-Flux water Heat Pipe Evaporator," Office of Naval Research, TR ME-62(73)ONR-012-2, Sept. 1973.

[12]Gibbs, W.J., Conformal Transformations in Electrical Engineering, Chapman and Hall Ltd., London, 1958, pp. 133-138.

[13]Prince, W.J., "Enhanced Tubes for Horizontal Evaporator Desalination Processes," M.S. Thesis, Univ. of California at Los Angeles, School of Engineering, 1971.